Nationaal Lucht- en Ruimtevaartlaboratorium
National Aerospace Laboratory NLR

NLR TP 97619

Large time step aero-structural coupling procedures for aeroelastic simulation

B.B. Prananta and M.H.L. Hounjet

DOCUMENT CONTROL SHEET

	ORIGINATOR'S REF.		SECURITY CLASS.
	TP 97619 U		Unclassified

ORIGINATOR
National Aerospace Laboratory NLR, Amsterdam, The Netherlands

TITLE
Large time step aero-structural coupling procedures for aeroelastic simulation

PRESENTED AT
CEAS International Forum on Aeroelesticity and Structural Dynamics, Rome, Italy, June 17-20, 1997.

AUTHORS	DATE	pp	ref
B.B. Prananta and M.H.L. Hounjet	973112	34	13

DESCRIPTORS

Aerodynamic forces	Euler equations of motion	Structural
Aeroelasticity	Finite volume method	
Computerized simulation	Fluid-solid interactions	
Computational fluid dynamics	Flutter analysis	
Computational grids	Navier-Stokes equation	
Dynamic structural analysis	Parallel processing (computer)	
	Structural dynamics	

ABSTRACT
Aero-structural coupling methods suitable for aeroelastic simulation involving large time steps are presented. Two methods are introduced and applied which are based on the extrapolation of the aerodynamic state and the structural state, both using gradient information from the equations and from the previous time steps, respectively. A new method is proposed based on the prognostication from a time-analysis of the time traces. Comparison of the methods with existing methods for several two-dimensional and three-dimensional cases show the supriority of the current schemes.

Summary

Aero-structural coupling methods suitable for aeroelastic simulation involving large time steps are presented. Two methods are introduced and applied which are based on the extrapolation of the aerodynamic state and the structural state, both using gradient information from the equations and from the previous time steps, respectively. A new method is proposed based on the prognostication from a time-analysis of the time traces. Comparison of the methods with existing methods for several two-dimensional and three-dimensional cases show the superiority of the current schemes.

Keywords Structural Dynamics, Aeroelasticity, CFD, Euler/ Navier-Stokes Equations, Fluid-Structure Interaction, Coupling Procedure, Time-Analysis

Contents

15 Figures

(34 pages in total)

1 Introduction

Methods for transonic aeroelastic simulation are being developed at the Delft University of Technology and the National Aerospace Laboratory in a joint research activity. Driven by the requirement of future industrial applications of these methods, special attention is devoted not only to a proper modeling of the physics but also to their efficiency and robustness. Consequently, an important practical aspect is the capability to march accurately at a large time step, thereby reducing the overall turn-around time. However, this implies that all components of the aeroelastic simulation methodology should possess a **large time step** capability.

In the past three years, the research was mainly focused on the development of an efficient time-accurate aerodynamic method for solving Euler/Thin-Layer Navier-Stokes equations. The resulting methods were reported in [1] and [2]. It was demonstrated that adequate results can be obtained using a time step of $\frac{\mathbf{O}(10)}{cycle}$, even for highly nonlinear flow conditions, involving significant shock trajectories and partly separated flow. A dynamic mesh algorithm suitable for large time step simulation which implies also large amplitude motion was also reported in [2]. For the robust transfer of data at the interface between aerodynamic and structural domains, a volume spline method was introduced in [3]. At present the attention is concentrated mainly on aero-structural coupling procedures.

The commonly used aero-structural method of [4] based on a simple extrapolation of aerodynamic forces turned out to be inadequate in the current research unless relatively small time steps are used. Therefore, an improvement of the coupling method is necessary to benefit from the large time step allowed by the current aerodynamic methods. Two coupling methods have been studied: an improved aerodynamic extrapolation method and a structural extrapolation method. Also a third one is introduced: the prognostic method. The latter is an extension of the structural extrapolation method and uses results of the time analysis to guess the new states.

In this paper the three coupling methods will be presented in detail. Results obtained for the NACA 64A010 in aeroelastic simulations are discussed. The results for the three-dimensional AGARD standard aeroelastic case of the 445.6 wing will also be presented to show the straightforward extension of the methods to more general n-DOF cases. The new methods turn out to improve the common method.

2 Aerodynamic Method

The aerodynamic model of the aeroelastic simulation method employs Euler/Thin-Layer Navier-Stokes equations. This model is suitable for the current study which concentrates on transonic flow. This section presents a short review of the method. More detailed descriptions of the present methods may be found in [1] and [2] for two-dimensional and three-dimensional configurations, respectively.

The governing equations are transformed from the Cartesian physical domain to a uniform computational domain as $\xi = \xi(x, y, z, t), \eta = \eta(x, y, z, t), \zeta = \zeta(x, y, z, t)$ and $\tau = t$ to facilitate the discretization. The conservative form of the Thin-Layer Navier-Stokes equations in a curvilinear coordinate system reads:

$$\frac{\partial \widehat{Q}}{\partial \tau} + \frac{\partial \widehat{E}}{\partial \xi} + \frac{\partial \widehat{F}}{\partial \eta} + \frac{\partial \widehat{G}}{\partial \zeta} = \frac{\partial \widehat{G}_v}{\partial \zeta}, \tag{1}$$

where $\widehat{Q} = hQ$ is the conservative variable and $(\widehat{E}, \widehat{F}, \widehat{G})$ are the inviscid fluxes in ξ, η, ζ directions. $\widehat{G}_v$ is the viscous term compatible with the thin-layer assumption. Closed with the equation of state and Fourier law of heat conduction, these equations can be solved for the flow variables. For turbulent flows the eddy viscosity concept is adopted and the algebraic turbulence model of Baldwin-Lomax is used to model the turbulent viscosity.

Eq.1 is spatially discretized using a cell-centered finite-volume method. Upwind methodology employing Roe's Flux Difference Splitting is applied for the inviscid flux. The viscous flux is discretized as usual in a central manner. An implicit multi-step method is employed for the temporal integration. Second or third order accurate backward differences are applied for the time derivative. The resulting discretized equations are solved using relaxation methods: symmetric line relaxation for two-dimensional cases and symmetric plane relaxation for three-dimensional cases. These methods are efficient and accurate for unsteady flow problems as was shown in [1] and [2].

The mesh deformation is handled using the spring analogy of Batina [5] employing an implicit method to solve the balance equation. The evaluation of the metrics is consistent with the geometric conservation law.

The parallelization of the three-dimensional aerodynamic method follows the domain decompo-

sition approach where each domain is assigned to a processor. Parallel Virtual Machine (PVM 3.3.11) routines are applied for communications among the processors. The parallel version of the code has been ported to a cluster of workstations and to MPP machines. The mesh is mapped to the processors in a two-dimensional way without decomposing the mesh in the normal direction. The effort to perform the parallelization was minor since the code running in each processor is essentially the serial code. The explicit part of this procedure somewhat slows down the convergence of the relaxation. So far this has not presented serious problems for the small to moderate number of processors (up to 32) applied in this study. Analysis is underway to asses this matter further.

3 Aeroelastic Method

In general the equation of motions for the aeroelastic system can be written as:

$$M\frac{d^2\mathbf{x}}{dt^2} + C\frac{d\mathbf{x}}{dt} + K\mathbf{x} = q_\infty S C_A(t, \mathbf{x}), \tag{2}$$

where M, C, and K are mass, damping and stiffness matrices, respectively. $\mathbf{x}$ represents a vector of natural coordinates, q_∞ is the freestream dynamic pressure, S is a reference area and C_A is the aerodynamic force coefficient which is governed by Eq.1. Eq.2 can be brought into a standard state space form:

$$\begin{aligned} \dot{X} &= AX + BU \\ A &= \begin{bmatrix} 0 & I \\ -M^{-1}K & -M^{-1}C \end{bmatrix}, B = \begin{bmatrix} 0 \\ q_\infty S \end{bmatrix} \end{aligned} \tag{3}$$

where $X = [\mathbf{x}, \dot{\mathbf{x}}]^T$ and $U = [C_A]$. When the aerodynamic forces do not depend on $\mathbf{x}$, a standard method can be use to solve Eq.3:

$$\begin{aligned} X^{n+1} &= \Phi X^0 + \int_0^{t(n+1)} \Phi(t-\tau) B U(\tau) d\tau \\ &\approx \Phi(\Delta t) X^n + \Theta(\Delta t)\bar{U}, \end{aligned} \tag{4}$$

where $\bar{U}$ is a representative value of $U(t)$ between time level (n) and $(n+1)$. Calculation of Φ and Θ can be found in e.g.[2][4]. To take into account the motion-dependent part of the aerodynamic forces many methods have been developed. Bendiksen [6] solved the aeroelastic equations in a fully coupled way using an explicit Runge-Kutta method. This is probably the ideal way according to the physical modeling. The main drawback is the small time step which has to be taken due to stability limits of the explicit method. This also has repercussions for the mesh to be regenerated/deformed and subsequently the calculation of metrics. The turn-around time of this method might be prohibitive for practical problems. An implicit method is rather difficult to construct since the gradient matrix has an unfavorable form, which might also lead to ill-conditioning [7]. A more recent method is due to Alonso and Jameson [8] who use an explicit method to drive a fully implicit method into convergence in each time step. This method needs mesh updates during the explicit iterations in each time step. This reduces the advantage of this method. The so-called loosely coupled method, or staggered method, or partitioned method is

more popular in solving Eq.2 due to the separation of the solution of aerodynamic and structural equations. The latter method has the advantage that it is suited for most of the methods developed for the flow and structural parts and in each time step a limited number of meshes have to be regenerated/deformed (in most cases only **one**). This is the main reason to employ the method in the present work. In the method an approximation of the aerodynamic force is constructed and used to evaluate the nonhomogeneous part of Eq.4. After the approximate position and the velocity on the surface have been obtained, these are used to enforce boundary conditions to the flow solver. The commonly used loosely coupled method can be found in [4], where the aerodynamic force is assumed to be $U = U(t)$. The aerodynamic force at time level $(n + \frac{1}{2})$ is then extrapolated as:

$$U^{n+\frac{1}{2}} \approx \frac{3}{2}U^n - \frac{1}{2}U^{n-1}. \tag{5}$$

This value is used to represent the value of U between time step (n) and $(n + 1)$. As mentioned previously this method fails to give good results for large time step simulations. Two approaches have been studied to improve the method:

Aerodynamic extrapolation The aerodynamic force is expressed as: $U = U(Q, X)$ and the extrapolation to time level $(n + \frac{1}{2})$ is:

$$U^{n+\frac{1}{2}} \approx U^n + (\frac{\partial U}{\partial Q}\frac{\partial Q}{\partial t} + \frac{\partial U}{\partial X}\frac{\partial X}{\partial t})\frac{\Delta t}{2}. \tag{6}$$

The $\partial Q/\partial t$ and $\partial X/\partial t$ are readily available data while $\partial U/\partial Q$ and $\partial U/\partial X$ have to be calculated.

Structural extrapolation The reason for this method is the fact that the structural part behaves smoother than the aerodynamic forces. Thus a better result may be expected from extrapolating the structural state. To obtain the aerodynamic force at time level $(n + \frac{1}{2})$, the state of the mesh is first approximated as:

$$X^{n+\frac{1}{2}} \approx X^n + \dot{X}^n\frac{\Delta t}{2}. \tag{7}$$

The $\dot{x}$ in the second term is readily available while the $\ddot{x}$ is approximated simply as $(\dot{x}^n - \dot{x}^{n-1})/\Delta t$. Using this data a mesh is generated and the surface velocity is used to enforce the boundary condition. Thus the aerodynamic part of the method marches at a time level between the structural states. This method is more efficient than the first one since all quantities needed for extrapolation are readily available or can be easily calculated. It should be noted that a similar method was introduced in [7] for a different reason, namely to satisfy

the GCL on the fluid-structure interface. It was concluded in [7] that the surface velocities had to be taken constant from time step (n) otherwise high frequency oscillation would occur due to violation of the GCL. In the present study, the velocity is linearly extrapolated from the former time steps. So far high frequency oscillation is not experienced. This may be explained from the fact that the GCL is satisfied by the aero solver, see [2].

Finally a prognostic method is proposed which is a refinement/generalization of the previous extrapolation methods and might be regarded as a high-order extrapolation using transfer functions[1]. In each time step the structural or aerodynamic part is extrapolated to the next time level by:

$$X^{(n+\frac{1}{2})} \approx P(X, U, t^{n+\frac{1}{2}}) \text{ or } U^{(n+\frac{1}{2})} \approx P(U, X, t^{n+\frac{1}{2}}).$$

Here $P(\#, t)$ denotes the approximation of the time trace $\{\#_n, \#_{n-1}.....\#_{n-m}\}$ at t which should be obtained by performing one of the analysis methods as presented in [9]. m denotes the number of retarded time steps in the time domain. It is obvious that as soon as the function P is not changing anymore the simulation can be stopped since the following time steps will not present any additional information. In fact this means the time step is virtually infinite.

3.1 Two-Dimensional Method

The motion of an rigid airfoil can be fully represented by two coordinates: $(h, \alpha)^T$, denoting the heave displacement of the elastic axis and rotation about the elastic axis, respectively. The formulation can be found in e.g. [1],[4]. Assuming that the h direction is parallel to z direction and pointing downward, the aerodynamic force coefficients are calculated as:

$$\begin{aligned} C_h &= -\frac{2}{M_\infty^2}\int p dS_z \approx -\frac{2}{M_\infty^2}\sum_i p_i \hat{\zeta}_{z,i}, \\ C_\alpha &= -\frac{2}{M_\infty^2}\int p(\mathbf{r}-\mathbf{r}_{EA})\times \mathbf{dS} \\ &\approx -\frac{2}{M_\infty^2}\sum_i p_i[(z-z_{EA})\hat{\zeta}_x - (x-x_{EA})\hat{\zeta}_z]_i, \end{aligned}$$

where p is the surface pressure nondimensionalized using $\rho_\infty a_\infty^2$. To obtain the relation of aerodynamic forces to the state variables, the coordinate on the surface is written as:

$$\begin{aligned} x^t &= x_{EA} + (x^0 - x_{EA})\cos\alpha + (z^0 - z_{EA})\sin\alpha \\ z^t &= z_{EA} - (x^0 - x_{EA})\sin\alpha + (z^0 - z_{EA})\cos\alpha - h/2, \end{aligned} \tag{8}$$

[1] Results of this method will be presented in a forthcoming publication

where superscript 0 represent mean steady position. Instead of using Q, p is used directly for the extrapolation of the aerodynamic forces. The required data for the extrapolation are:

$$\begin{aligned}
\frac{\partial C_h}{\partial p}\frac{\partial p}{\partial t} &= \left.\frac{\partial C_h}{\partial t}\right|_{h,\alpha} = -\frac{2}{M_\infty^2}\sum_i \frac{\partial p_i}{\partial t}\hat{\zeta}_{z,i}, \\
\frac{\partial C_h}{\partial \alpha} &= -\frac{2}{M_\infty^2}\sum_i p_i(-\hat{\zeta}_z^0 \sin\alpha - \hat{\zeta}_x^0 \cos\alpha)_i, \\
\frac{\partial C_h}{\partial h} &= \frac{\partial C_h}{\partial \dot{h}} = \frac{\partial C_h}{\partial \dot{\alpha}} = 0.
\end{aligned}$$

The gradient of the moment C_α is calculated in a similar manner except:

$$\begin{aligned}
\frac{\partial C_\alpha}{\partial p}\frac{\partial p}{\partial t} &= \left.\frac{\partial C_\alpha}{\partial t}\right|_{h,\alpha} = -\frac{2}{M_\infty^2}\sum_i \frac{\partial p_i}{\partial t}[(z-z_{EA})\hat{\zeta}_x - (x-x_{EA})\hat{\zeta}_z]_i, \\
\frac{\partial C_\alpha}{\partial \alpha} &= -\frac{2}{M_\infty^2}\sum_i p_i[(z-z_{EA})\frac{\partial \hat{\zeta}_x}{\partial \alpha} + \frac{\partial z}{\partial \alpha}\hat{\zeta}_x - (x-x_{EA})\frac{\partial \hat{\zeta}_z}{\partial \alpha} - \frac{\partial x}{\partial \alpha}\hat{\zeta}_z]_i, \\
\frac{\partial C_\alpha}{\partial h} &= \frac{\partial C_\alpha}{\partial \dot{h}} = \frac{\partial C_\alpha}{\partial \dot{\alpha}} = 0.
\end{aligned}$$

$\partial\hat{\zeta}_x/\partial\alpha, \partial\hat{\zeta}_z/\partial\alpha, \partial x/\partial\alpha$ and $\partial z/\partial\alpha$ can be easily calculated from Eq.8. Inserting these formula in Eq.6 the aerodynamic forces can then be predicted using X and $\dot{p}$ data.

3.2 Three-Dimensional Method

The structural part in the three-dimensional method is represented by a finite number of approximate modes. These modes are obtained from equation:

$$M\frac{d^2\mathbf{x}}{dt^2} + K\mathbf{x} = 0,$$

which is solved using a finite element package to obtain the mode shapes ϕ_i and eigenfrequencies ω_i. The resulting mode shapes are normalized w.r.t. the mass matrix. Substitution of:

$$\mathbf{x} = \phi\mathbf{q},\ \phi^T M\phi = I,\ \phi^T K\phi = \omega_i,$$

results in an independent set of equations (neglecting the stuctural damping):

$$\frac{d^2 q_i}{dt^2} + \omega_i^2 q_i = q_\infty S Q_i,\ i = 1..\mathrm{N},$$

where Q_i is the nondimensional generalized force defined as:

$$Q_i = \frac{1}{S}\int_S p\phi dS.$$

N represents a limited number of modes which are employed in the computation. Most of the time N is much smaller than the number of degrees of freedom employed in the finite element calculation. In the present work only the z displacement of the mode shape ϕ is used since in practice the displacement in the other directions are usually very small. This leaves the calculation of the generalized forces independent from the generalized coordinates implying that the present aerodynamic extrapolation method is equal to the original method of [4]. Thus for the three-dimensional case only the structural extrapolation method is considered. The CPU time used for the calculation of the structural part is small compared to the one for the aerodynamic part. This is mainly due to the relatively small number of DOF's taken for the analysis. In the present version of the method, the calculation of the structural part is carried out in the coordinating processor.

4 Results

The applicability range of the method is directed to two-dimensional and three-dimensional cases. In the present paper only results employing Euler equations are considered, since from accuracy reasons these allow the largest time steps to be taken. The examples in this paper focus on aeroelastic applications in 2-D and 3-D and demonstrate the status of the CAS method.

4.1 Two-dimensional

The well-known Isogai case A [10] is considered for the two-dimensional test case. The structural parameters are a=-2.00, x_α=1.80, r_α^2=3.48 μ=60.00 and the ratio of the uncoupled frequency ω_h/ω_α=1.00. The flutter boundaries of this case using the present method, compared to some other methods, have already been shown in [1]. The result presented here will concentrate on the large time step aspect of the method. A mesh consisting of 140$\times$32 points was applied. The simulation is started from a steady condition with an initial $\dot{x}$. The small time step simulation uses $\frac{\mathbf{32}\ time\ steps}{cycle}$ of the uncoupled mode while the large time step simulation applies $\frac{\mathbf{8}\ time\ steps}{cycle}$.

Two cases are considered, the first one is a supercritical condition at M_∞=0.775 with $V^* = U_\infty/(\omega_\alpha b\sqrt{\mu})$=1.00 and the second one is a subcritical condition at M_∞=0.80 with V^*=0.53.

Applying the small time step for the supercritical case, the common aerodynamic extrapolation of [4], the present aerodynamic extrapolation and the present structural extrapolation methods converge to the same results.

The comparison of simulation results using small and large time steps are presented in Fig. 1–3. Fig. 1 reveals clearly the inadequacy of the common method for large time step simulations. On the other hand the results of the present aerodynamic extrapolation method, depicted in Fig. 2, show a good agreement with the small time step simulations. Fig. 3 shows that similar good comparisons are obtained using the structural extrapolation method. After analyzing the time traces using the fitting method of [9], a more obvious comparison can be observed:

method	$\bar{\lambda}$	V^*	CPU (mins)	time step
present aerodynamic	0.00616	0.942	46	small ($\frac{\mathbf{32}}{cycle}$)
present aerodynamic	0.00617	0.942	15	large ($\frac{\mathbf{8}}{cycle}$)
present structural	0.00679	0.938	15	large ($\frac{\mathbf{8}}{cycle}$)
classical	*0.01270*	*0.911*	*15*	*large* ($\frac{\mathbf{8}}{cycle}$)

where $\bar{\lambda}$ is the damping decay coefficient. Note that the classical method eventually produces

flutter speed which is about 5% lower than the rest.

The simulations using small time step needed 46 minutes of CPU time on a SGI R8000 workstation, while large time step simulations needed 15 minutes, which is a significant saving of turn-around time. It should be noted that although the time step is four times larger, the speed-up of the large time step simulation is less than four because more subiterations are required per time step.

A similar exercise has been performed for the subcritical case where a strong shock wave is present. The results are shown in Fig. 4–6. Similar observations can be made as for the supercritical example. At the large time step the current methods are superior to the common aerodynamic extrapolation method of [4] ,although the latter performs much better in this case. A more detail comparison after analysis of the time traces is:

method	λ	V^*	CPU (mins)	time step
present aerodynamic	-0.00167	0.541	46	small ($\frac{32}{cycle}$)
present aerodynamic	-0.00167	0.541	15	large ($\frac{8}{cycle}$)
present structural	-0.00146	0.540	15	large ($\frac{8}{cycle}$)
classical	*+0.00172*	*0.528*	*15*	*large* ($\frac{8}{cycle}$)

Note that the classical method produces unstable result while the rest produce stable ones.

4.2 Three-dimensional

The well-known three-dimensional AGARD standard aeroelastic configuration is considered. This configuration is described in [11]. The configuration for dynamic response I wing 445.6 model *weakened no.3* is selected. The grid applied for this calculation consists of 121$\times$29$\times$24 mesh points. The case at M_∞=0.96 with $\mu = 225.820$ is considered. It should be noted that this value of μ is only consistent at the experimental flutter point which was obtained at V^*=0.3076. In the present calculation it is used for the whole simulation. To show the applicability of the present aerodynamic method for large time step simulations a forced vibration case is first considered. The second mode of 445.6 wing is excited in a sinusoidal motion with reduced frequency k=0.10, based on root semi-chord, and an amplitude of 0.005. Fig. 7 shows the response of the first two vibration modes using a small time step ($\frac{48}{cycle}$) and a large time step ($\frac{10}{cycle}$). No significant differences have been found . The CPU time for the small time step simulation is about 120 minutes/cycle using one processor of the CRAY J90 or 20 minutes/cycle, using a cluster of 4 SUN ULTRA SPARC workstations. The large time step simulation on the CRAY and the SUN takes about 60 and 12.5 minutes/cycle, respectively. Next the validation of the structural extrapolation method is presented. For this purpose the first 2 vibration modes are used, namely the first bending

and first torsion modes. These modes are primarily involved in the flutter mechanism [12]. To cross-check the methods, simulations with the aerodynamic extrapolation method of [4] and the present structural extrapolation method were applied using a small time step ($\frac{48}{cycle}$) of the second mode. The results of both methods showed an excellent agreement.

For the large time step simulation $\frac{8 steps}{cycle}$ of the second mode is employed. The comparison of the results for the aerodynamic extrapolation method of [4] is shown in Fig. 8. As already noted for the two-dimensional case the method is not adequate for large time step simulations. The results obtained with the current structural extrapolation method at the large time step show in general a good agreement with the results obtained with the of small time step simulation. The comparison of the value of damping decay coefficients is:

method	$\bar{\lambda}$	CPU (mins)	time step
present structural	0.0040	40	small ($\frac{48}{cycle}$)
present structural	0.0042	25	large ($\frac{8}{cycle}$)
classical	*0.0102*	*25*	*large* ($\frac{8}{cycle}$)

Finally the present structural extrapolation method is employed for a simulation involving 4 vibration modes. The time step is set at $\frac{8}{cycle}$ of the highest modes. Three runs were made at V^*=0.253, V^*=0.266 and V^*=0.293. The time response of the first 2 modes is depicted in Fig. 10. The flutter speed index is calculated from the interpolation of damping data. The comparison with data available from other references is shown in the table below:

Method	V^*
Experiment [11]	0.3076
CFL3D (EE-NS) [12]	0.256-0.287
AESIM (FP) [13]	0.303
Present (EE)	0.279

Is should be noted that the result of CFL3D was estimated from [12]. The CPU time for each simulation is about 18 minutes/cycle on a cluster of 4 SUN ULTRA SPARC workstations.

4.3 Work in progress

The present method has been applied to a more realistic configuration for aerospace applications. Fig. 11 shows a mesh with about 200,000 points around a fighter-type configuration. The inlet of the engine has been smoothed. The case considered is a transonic condition at M_∞=0.92 and α_{mean}=6.00. All results were obtained using the Euler mode. Fig. 12 shows the pressure contour on the surface of the aircraft.

The comparison of the pressure on the upper surface of the wing between the present result and the experimental data is presented in Fig. 13. The overall agreement is good except at the shock and tip region. The latter may be explained by the fact that the experimental result was obtained using a wind tunnel model having a tip-launcher, while the present calculation was carried out without one. The shock which is too strong may be improved by using the Navier-Stokes equations.

An unsteady case is considered which is a torsion mode oscillation with an amplitude of α_{amp}=0.50. Fig. 14 and Fig. 15 show the real and imaginary part of of the pressure on the upper surface of the wing compared to the experimental results obtained in the NLR High Speed Tunnel. Two runs were made employing small and large time steps on a SUN MP using 6 processors out of maximum 8. The small time step ($\frac{64}{cycle}$) required 3 hours/cycle of wall-clock time and the large time step ($\frac{8}{cycle}$) required 25 minutes/cycle of wall-clock time. In general the small time step results as well as the large time step results show a good agreement with the experimental data.

5 Concluding Remarks

In this paper the status of the TU Delft system for aeroelastic simulation has been presented and demonstrated.

Attention has been given to simple and fast fluid structure coupling procedures. The procedures are based on the extrapolation of the aerodynamic state, the structural state and/or both using gradient information from the equations, from the previous time steps or from the prognostics obtained from a time-analysis of the time traces.

The parallelization of the three-dimensional aerodynamic solver has been described.

The two-dimensional and three-dimensional applications have led to the following observations:

- Accurate results can be obtained with time steps as large as $\frac{8}{cycle}$.
- Flutter boundaries can be obtained in acceptable turn-around times on a cluster of current workstations.
- Flutter boundaries compare fairly well with data provided by other methods and the experiment.
- A significant computer cost reduction of more than 60% is obtained by the embedding of the current extrapolation schemes which allow for the large time step simulations.

Finally it can be concluded that the affordability of the present method is increased.

6 Acknowledgment

The authors would like to mention Prof. R.J. Zwaan and Prof. H.W.M. Hoeijmakers for valuable discussions and support. Mr. Prananta's stay in The Netherlands is sponsored by the RI-NL APERT project. TU Delft Center for High Performance Applied Computing (HPαC) is acknowledged for granting computing time on CRAY J90 and CRAY T3E-600 computers.

7 References

1. B.B. Prananta, M.H.L. Hounjet, and R.J. Zwaan. "A Thin-Layer Navier Stokes solver and its applications for aeroelastic analysis of an airfoil in transonic flows". In *Proceedings of 1995 International Forum on Aeroelasticity and Structural Dynamics*, pages 15.1–15.15, Manchester, June 1995. Royal Aeronautical Society.
2. B.B. Prananta and M.H.L. Hounjet. " Aeroelastic Simulation with Advanced CFD Methods in 2-D and 3-D Transonic Flow". In *Proceedings of 1996 Unsteady Aerodynamics Conference* , pages 7.1–7.14, London, July 1996. Royal Aeronautical Society.
3. M.H.L. Hounjet and J.J. Meijer. "Evaluation of Elastomechanical and Aerodynamic Data Transfer Methods for Non-planar Configurations in Computational Aeroelastic Analysis". In *Proceedings of 1995 International Forum on Aeroelasticity and Structural Dynamics*, pages 11.1–11.24, Manchester, June 1995. Royal Aeronautical Society.
4. J.W. Edwards, R.W. Bennett, W. Whitlow Jr, and D.A. Seidel. "Time marching transonic flutter solutions including angle of attack effects". AIAA Paper 82-0685, AIAA, 1982.
5. J.T. Batina. "Unsteady Euler algorithm with unstructured dynamic mesh for complex- aircraft aeroelastic analysis". AIAA Paper 89-1189, AIAA, April 1989.
6. O.O. Bendiksen. "A new approach to computational aeroelasticity". AIAA Paper 91-0939-CP, AIAA, 1991.
7. C. Farhat and M. Lesoinne. "On the accuracy, stability and performance of the solution of three-dimensional nonlinear transient aeroelastic problems by partitioned procedures". AIAA Paper 96-1388-CP, AIAA, 1996.
8. J.J. Alonso and A. Jameson. "A Fully-implicit time-marching aeroelastic solution". AIAA Paper 94-0056, AIAA, 1994.
9. M.H.L. Hounjet, B.J.G. Eussen and M.W. Soijer. " Analysis of Computational Aeroelastic Simulations by Fitting Time Signals" In Proceedings CEAS Symposium: International Forum on Aeroelasticity and Structural Dynamics, CEAS, Rome, June 17-20 1997.
10. K. Isogai. " On the transonic dip mechanism of flutter of a sweptback wing". *AIAA Journal*, 7:793–795, July 1979.
11. E.C. Yates Jr. "AGARD standard aeroelastic configurations for dynamic response, I-wing 445.6". Report 765, AGARD, July 1988.
12. E.M. Lee-Rausch and J.T. Batina. "Calculation of AGARD wing 445.6 flutter using Navier-Stokes aerodynamics". AIAA Paper 93-3476, AIAA, August 1993.
13. M.H.L. Hounjet and B.J.G. Eussen. "Outline and application of the NLR aeroelastic simulation method". ICAS Paper 94-5.8.2, ICAS, September 1994.

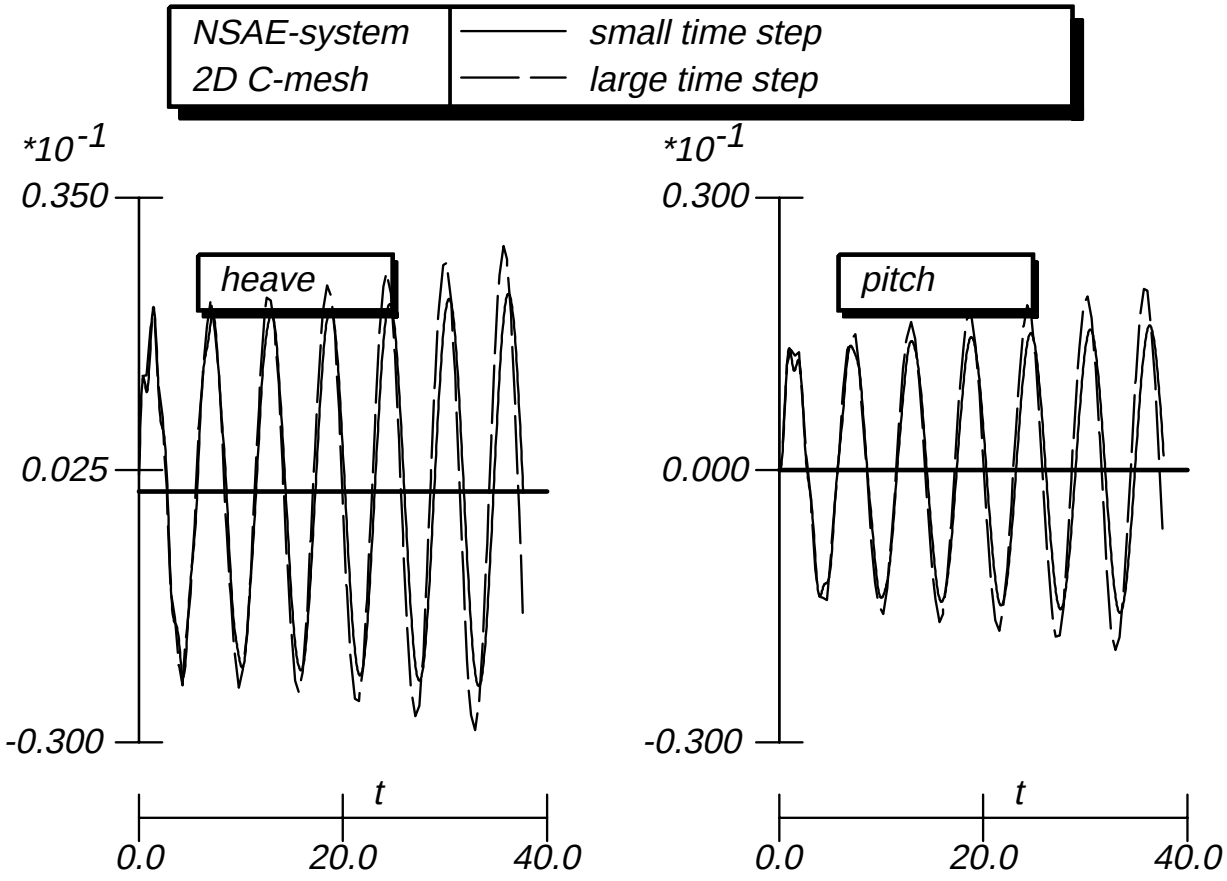

Fig. 1 Comparison of time responses between small ($\frac{32}{cycle}$) and large ($\frac{8}{cycle}$) time steps simulation for extrapolation method of [4], Isogai case A at M_∞=0.775

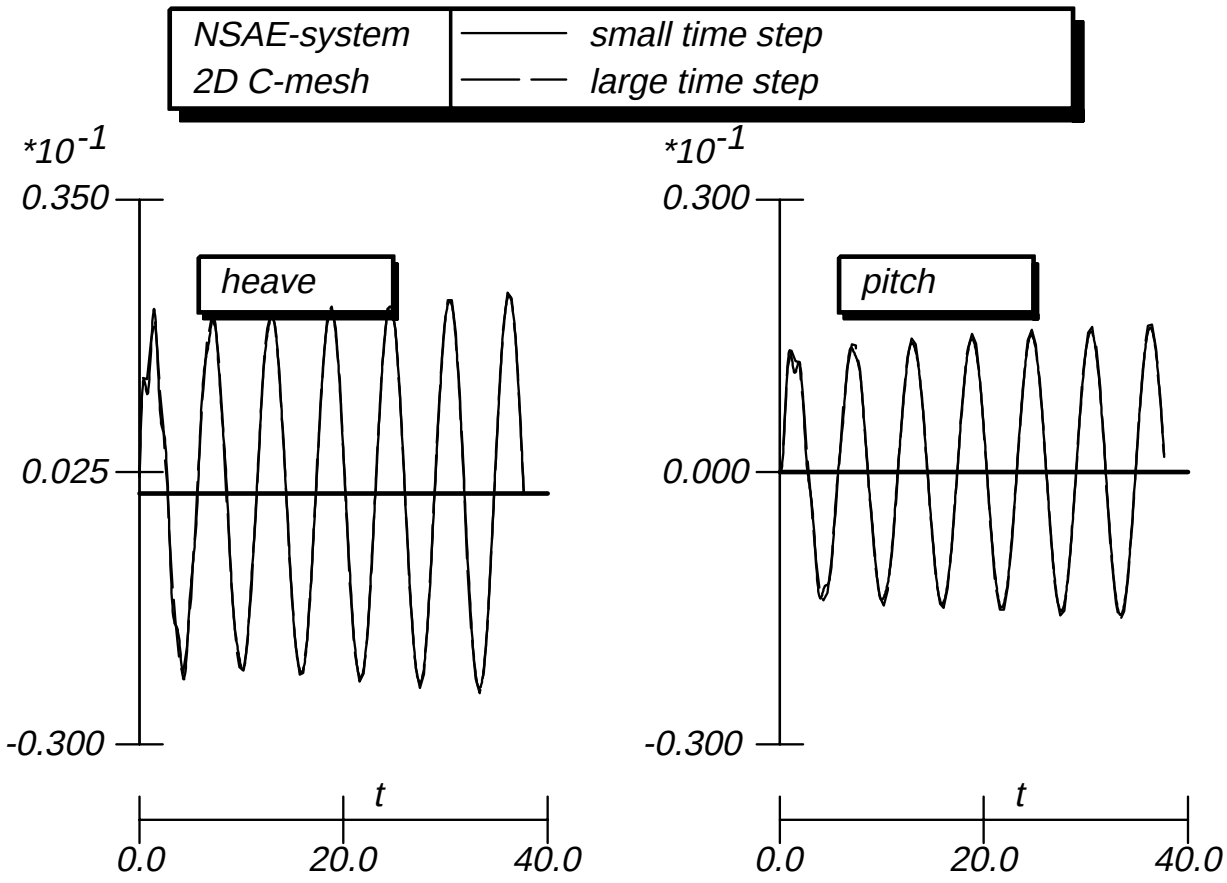

Fig. 2 Comparison of time responses between small ($\frac{32}{cycle}$) and large ($\frac{8}{cycle}$) time steps simulation for the present aerodynamic extrapolation method, Isogai case A at M_∞=0.775

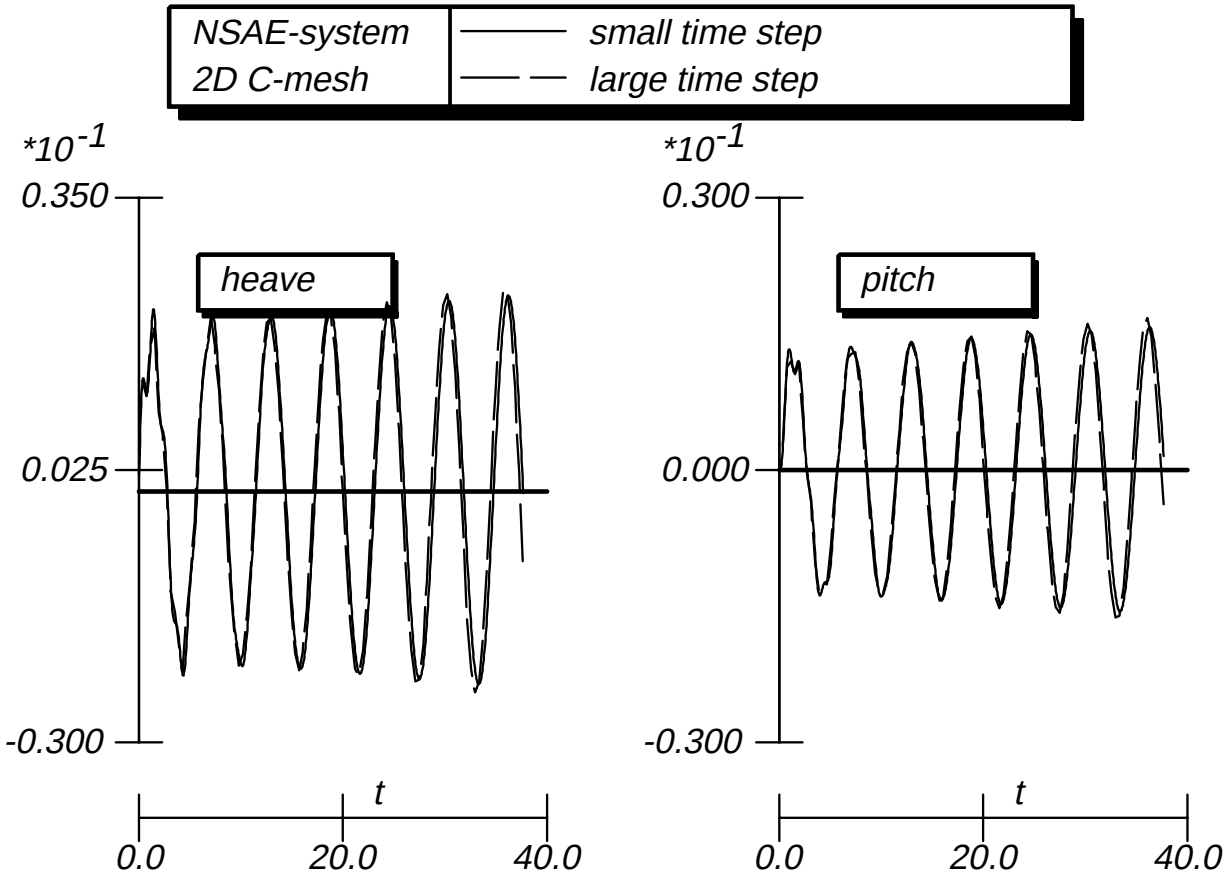

Fig. 3 Comparison of time responses between small ($\frac{32}{cycle}$) and large ($\frac{8}{cycle}$) time steps simulation for the present structural extrapolation method, Isogai case A at M_∞=0.775

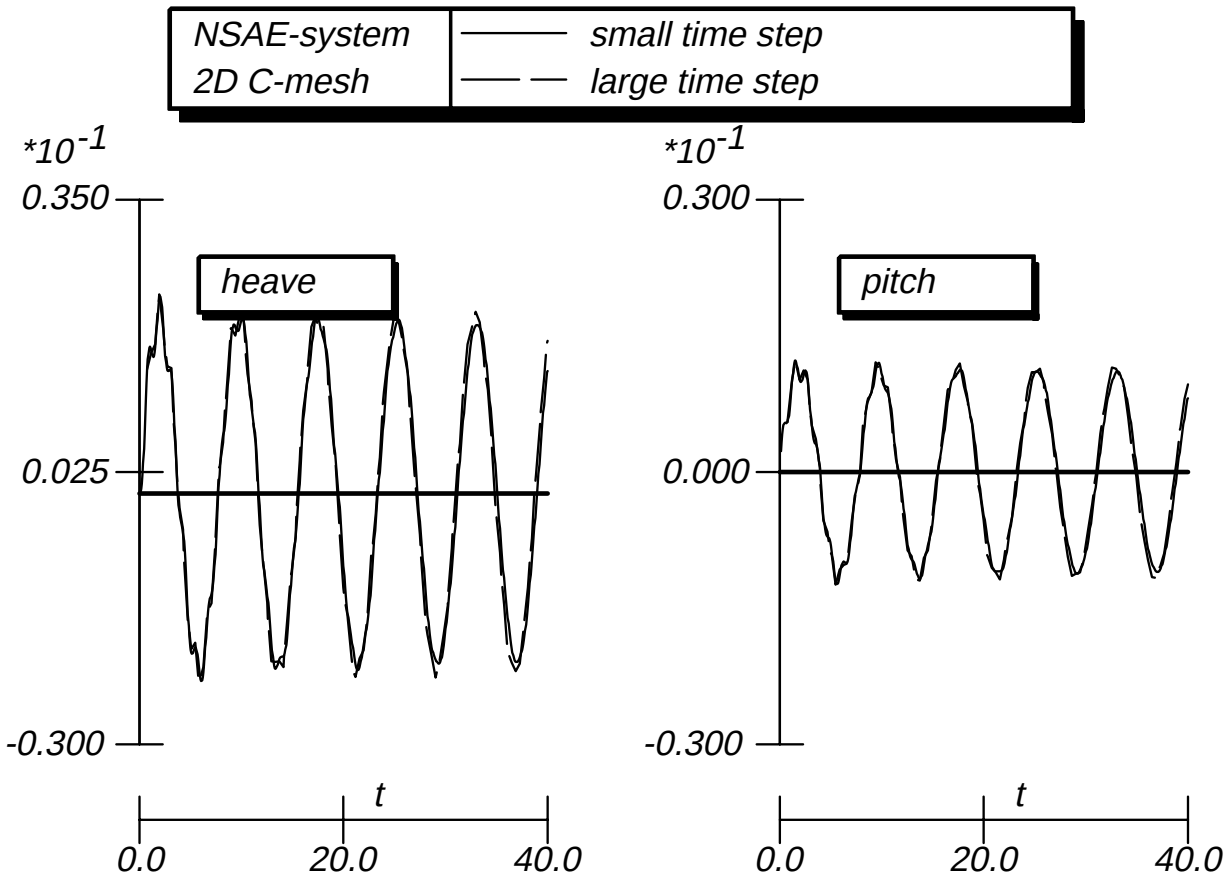

Fig. 4 Comparison of time responses between small ($\frac{32}{cycle}$) and large ($\frac{8}{cycle}$) time steps simulation for aerodynamic extrapolation method of [4], Isogai case A at M_∞=0.85

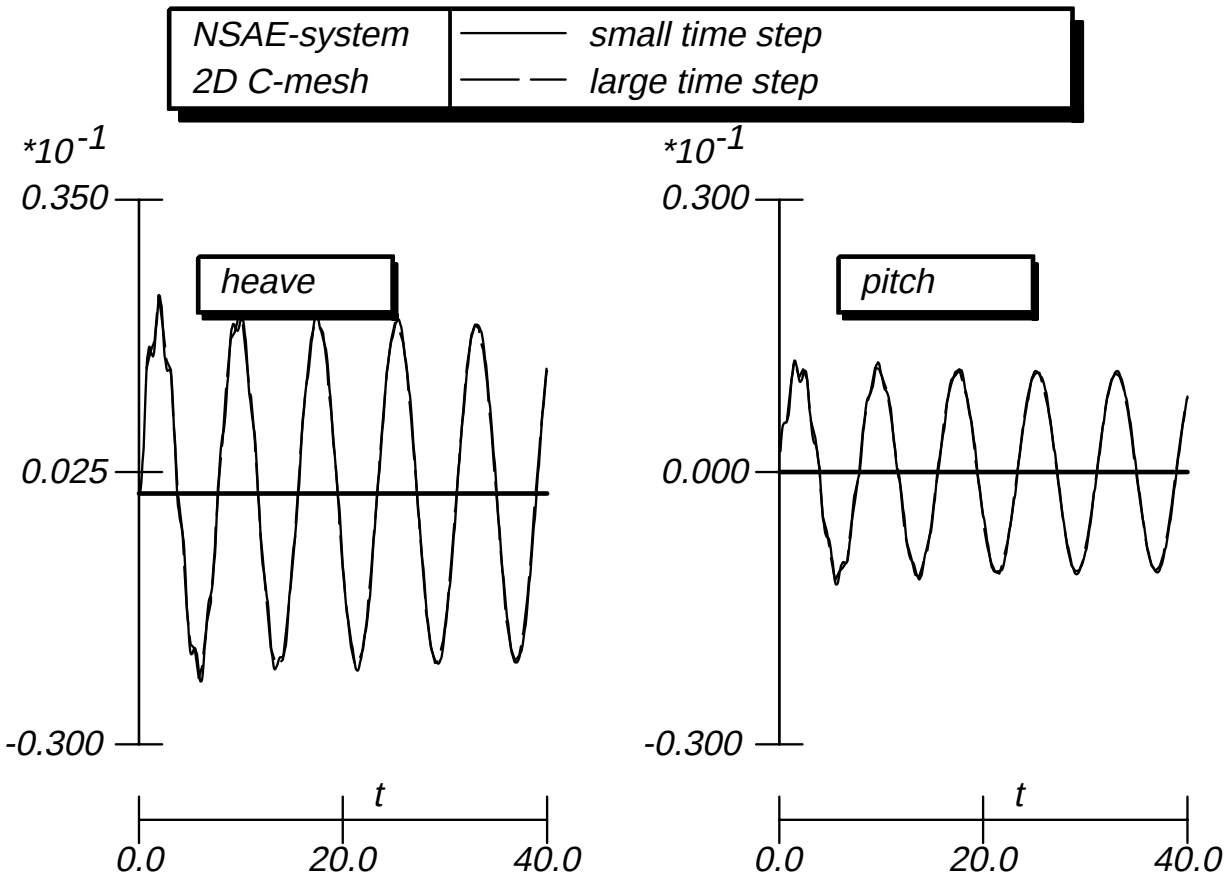

Fig. 5 Comparison of time responses between small ($\frac{32}{cycle}$) and large ($\frac{8}{cycle}$) time steps simulation for the present aerodynamic extrapolation method, Isogai case A at M_∞=0.85

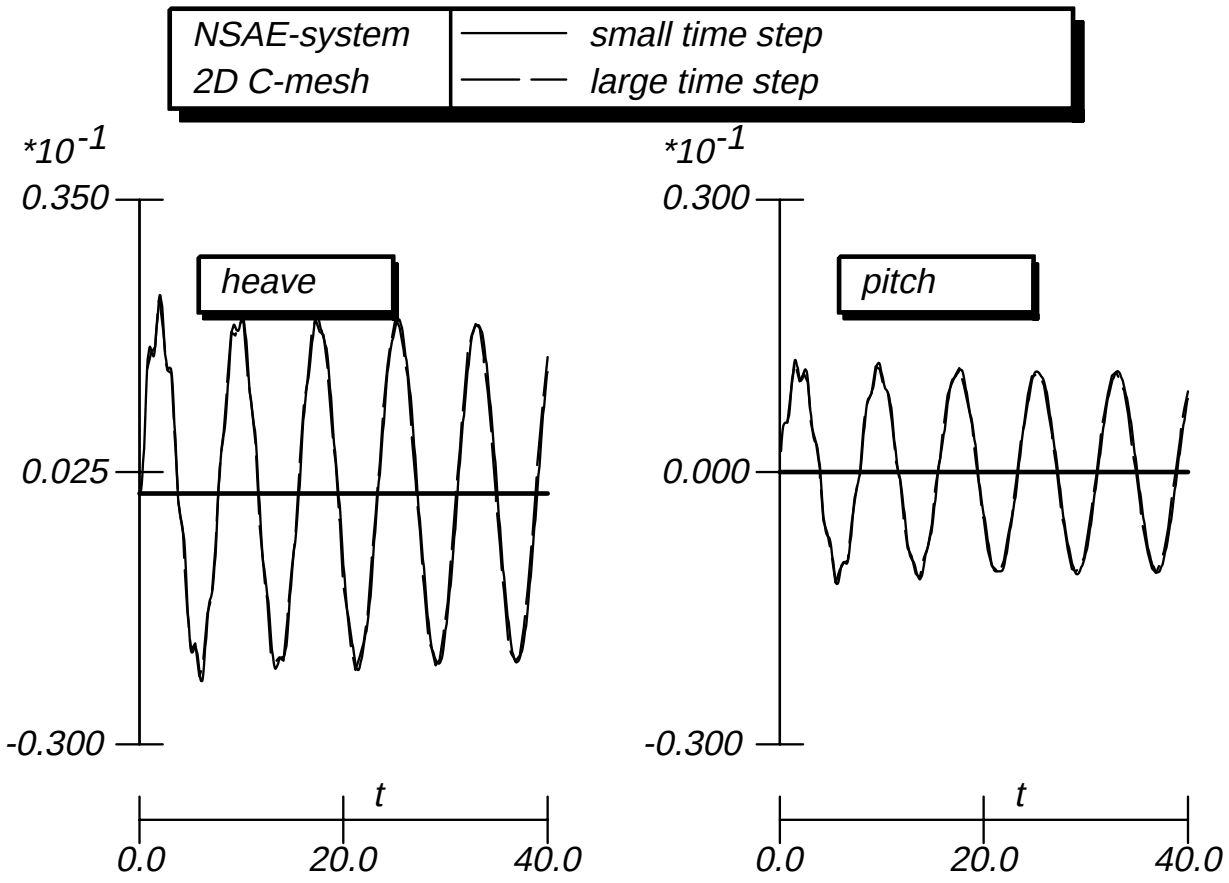

Fig. 6 Comparison of time responses between small ($\frac{32}{cycle}$) and large ($\frac{8}{cycle}$) time steps simulation for the present structural extrapolation method, Isogai case A at M_∞=0.85

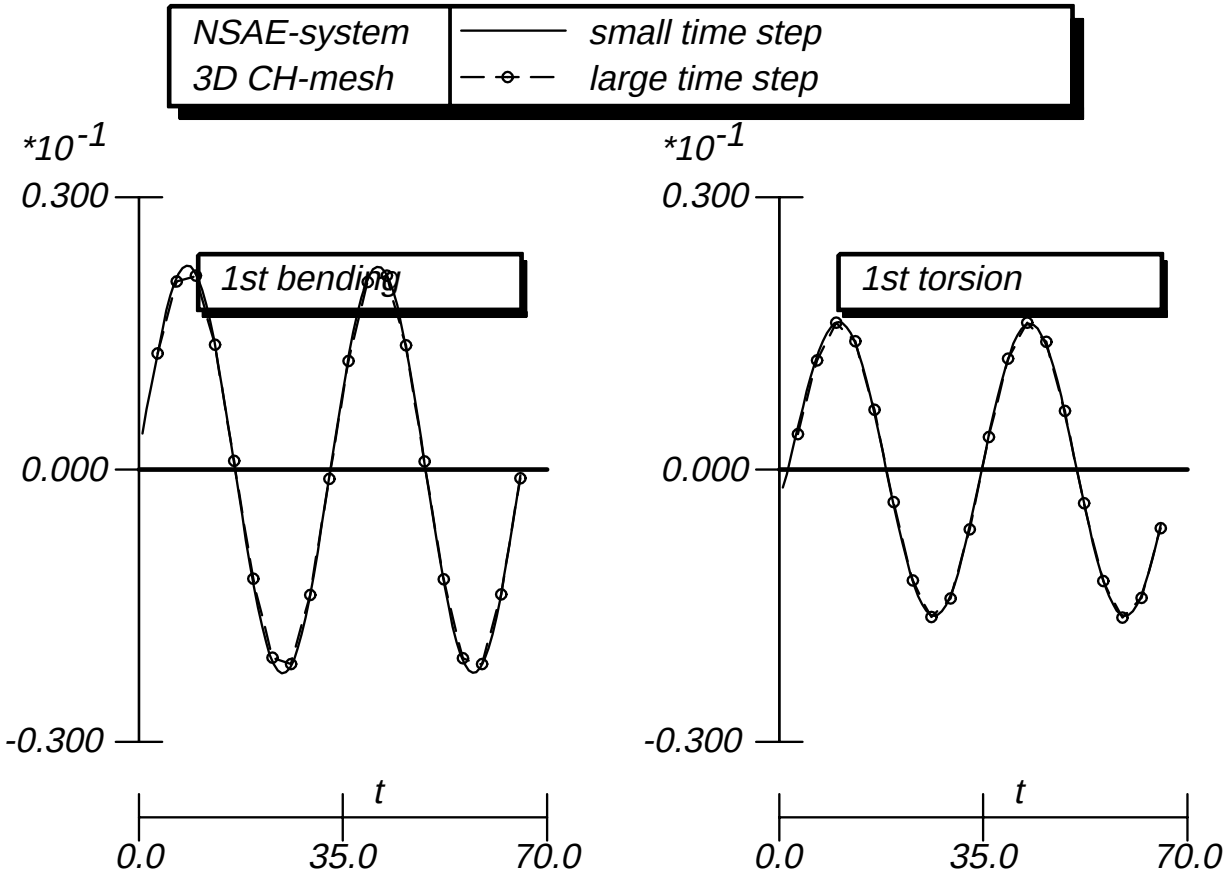

Fig. 7 Comparison of forced vibration case of 445.6 wing at M_∞=0.96 between small ($\frac{48}{cycle}$) and large ($\frac{10}{cycle}$) time steps runs

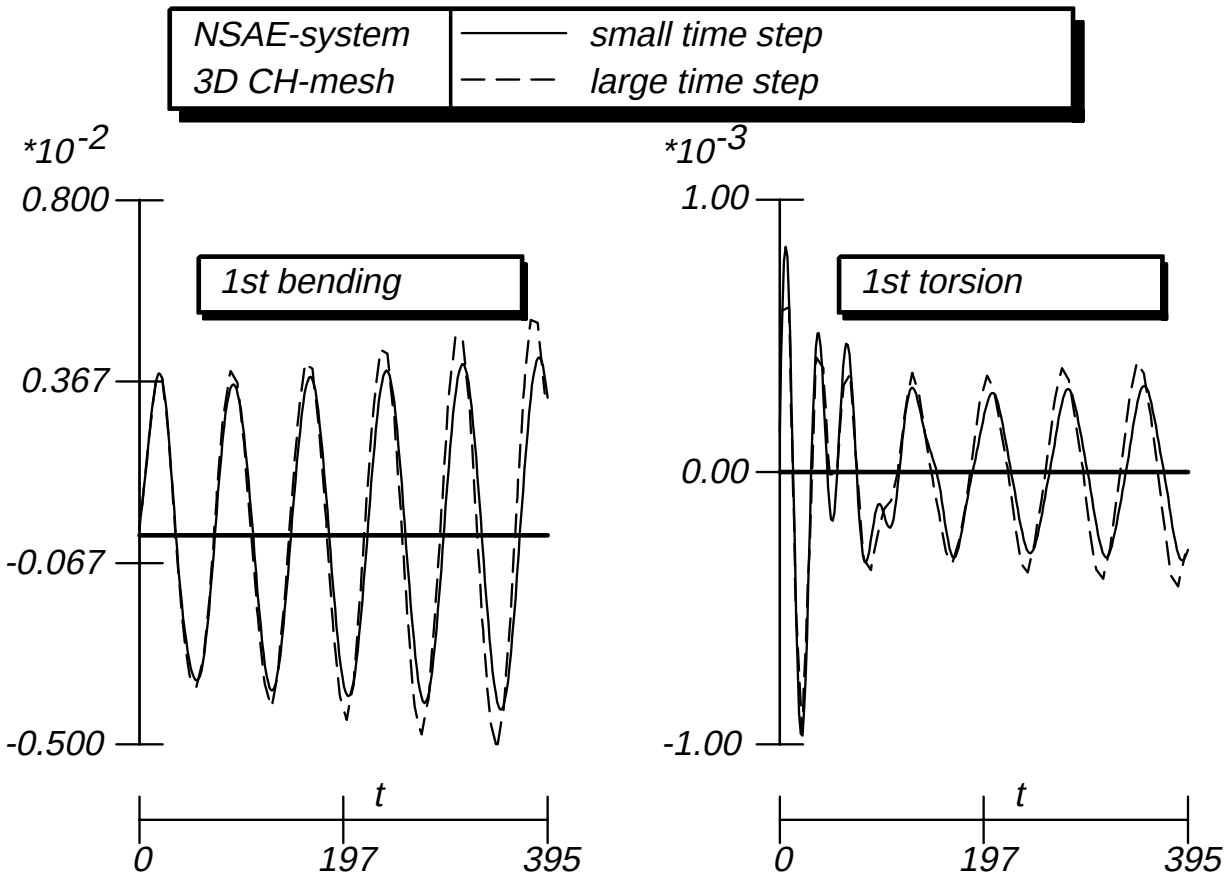

Fig. 8 Comparison of time responses between small ($\frac{48}{cycle}$) and large ($\frac{8}{cycle}$) time steps simulation for aerodynamic extrapolation method of [4], 445.6 wing at M_∞=0.96

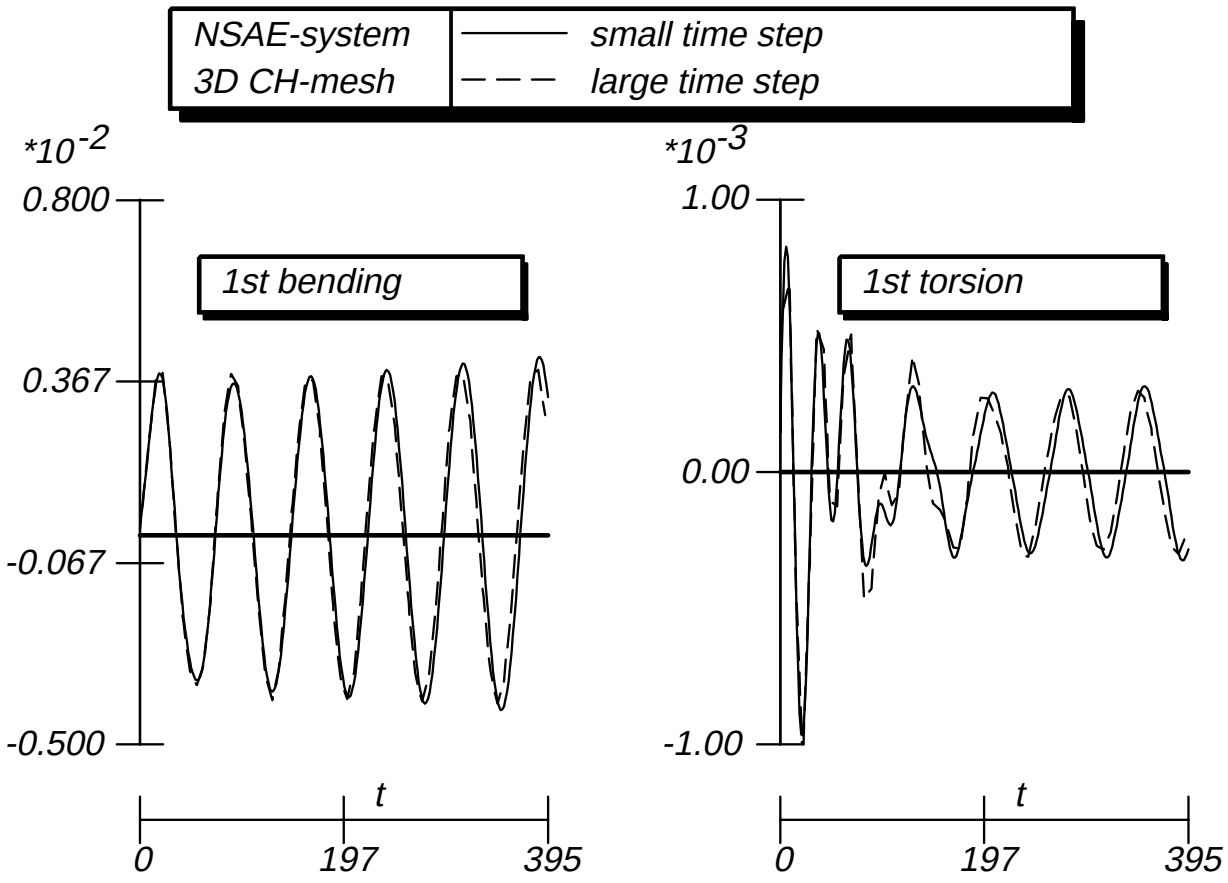

Fig. 9 Comparison of time responses between small ($\frac{48}{cycle}$) and large ($\frac{8}{cycle}$) time steps simulation for the present structural extrapolation method, 445.6 wing at M_∞=0.96

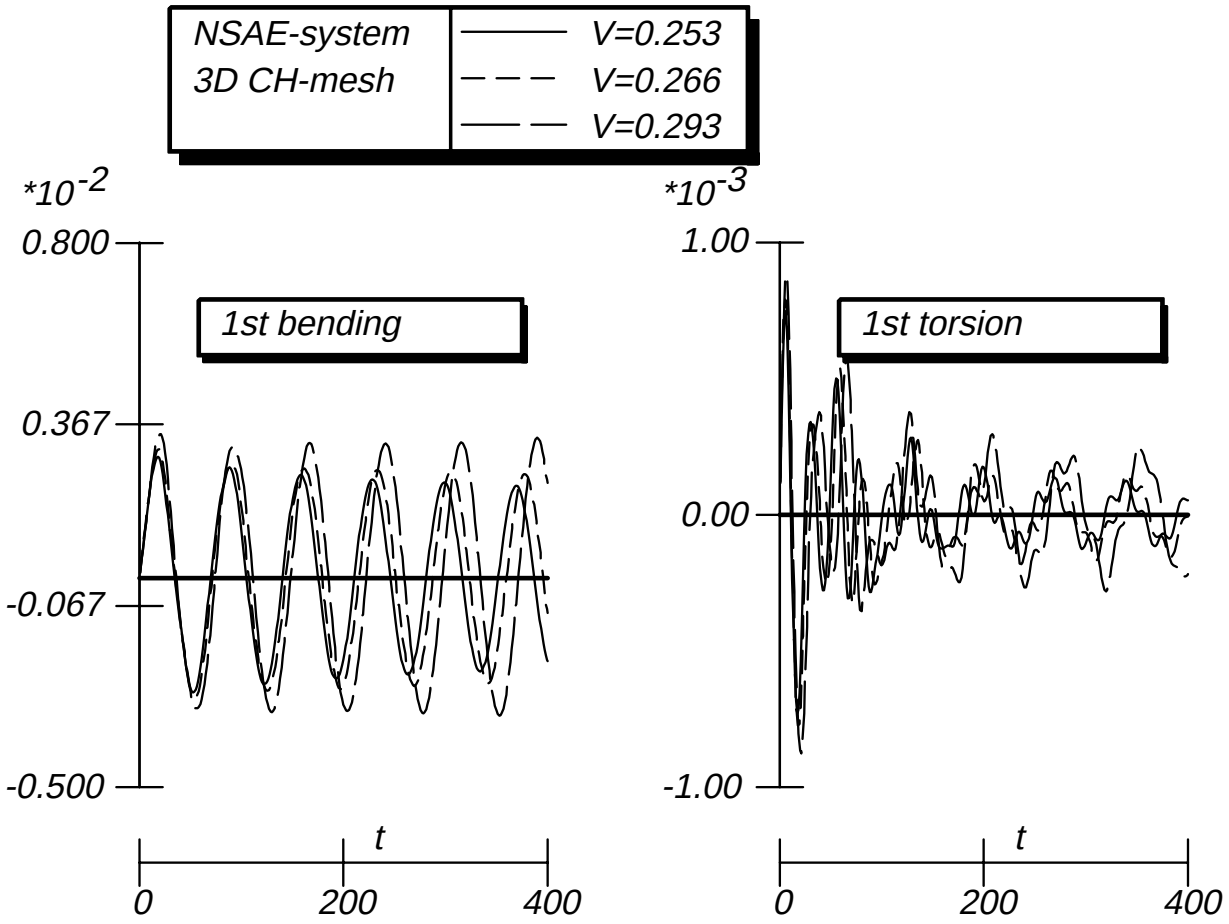

Fig. 10 Time responses of the first two modes of 445.6 wing at M_∞=0.96 for three speed indices

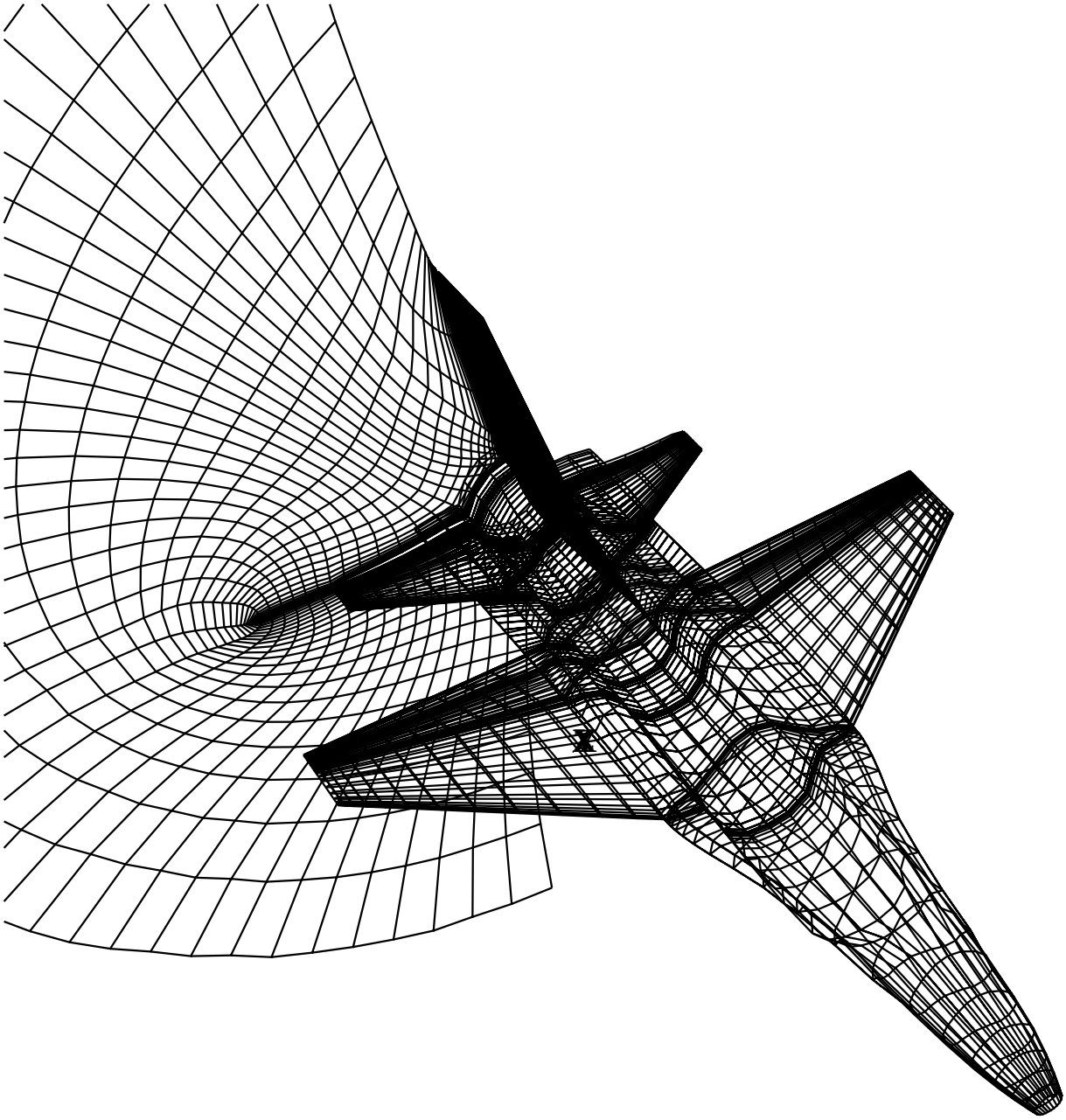

Fig. 11 Mono-block HO topology mesh around wing-body-tail fighter type configuration, number of points ~200,000.

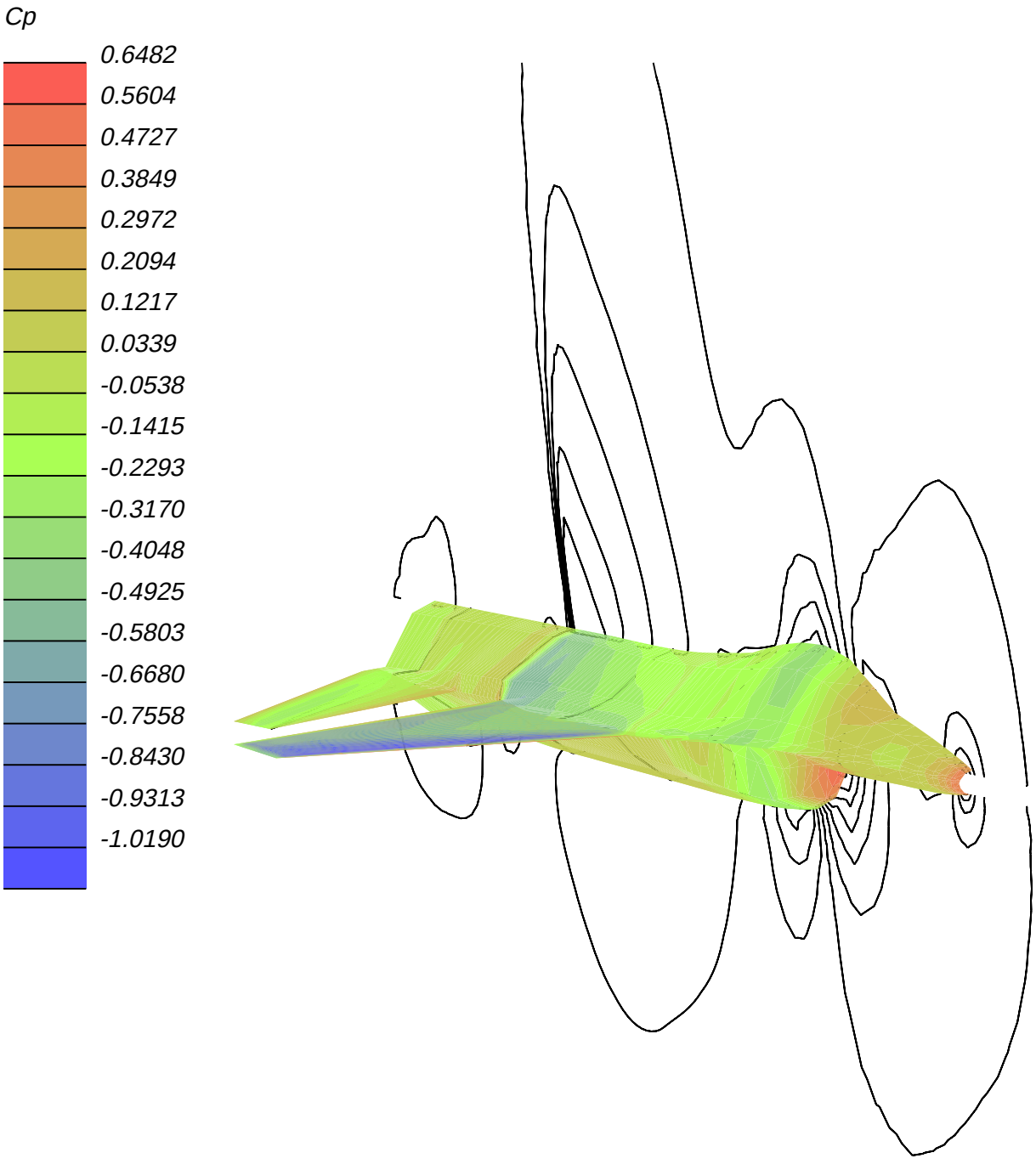

Fig. 12 Steady pressure contour on fighter type configuration at $M_\infty = 0.92$, $\alpha = 6.00$

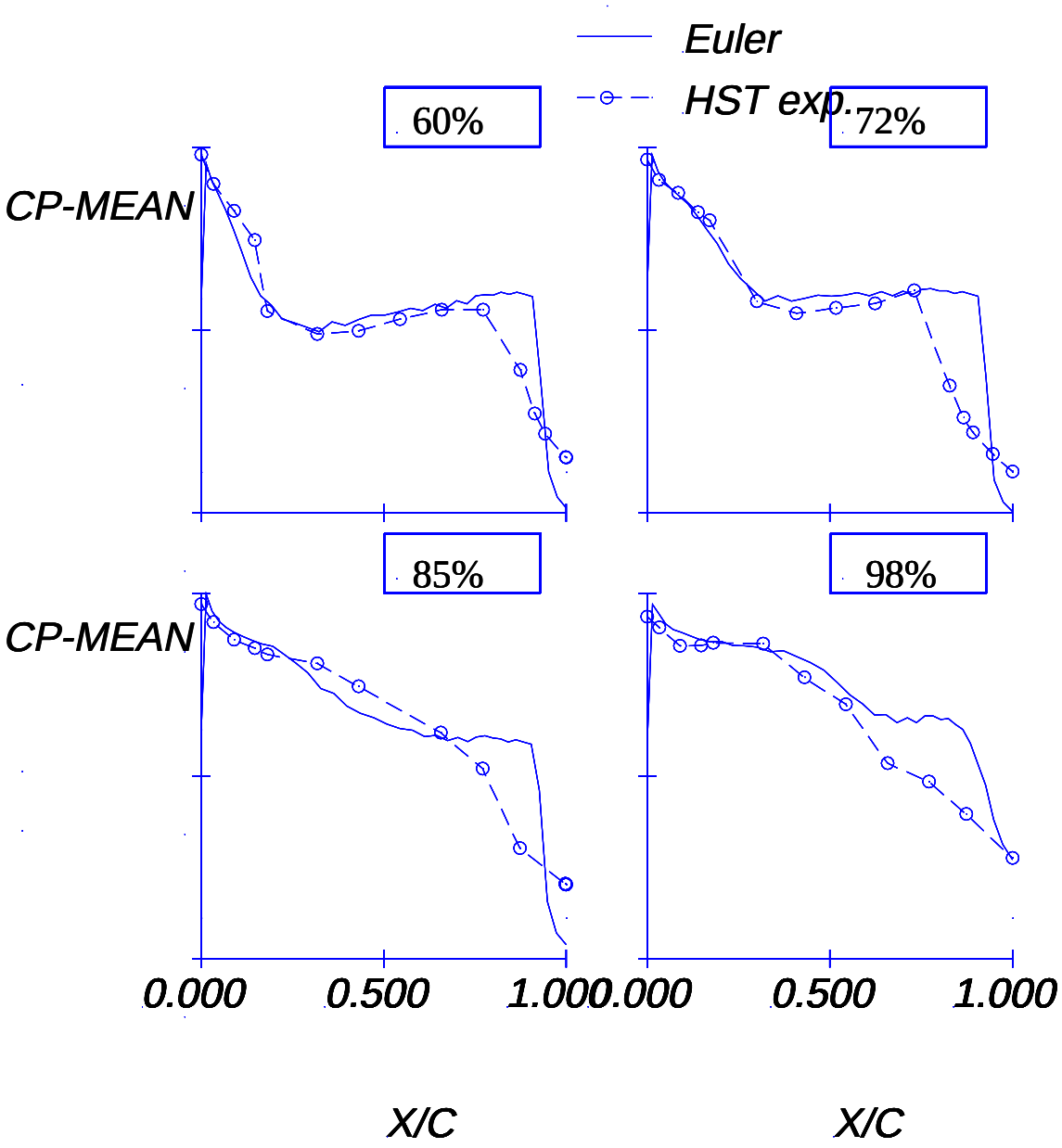

Fig. 13 Comparison of experimental and calculated mean steady pressure distributions on wing of fighter type configuration at $M_\infty = 0.92$, $\alpha = 6.00$, $\alpha_{amp} = 0.50$

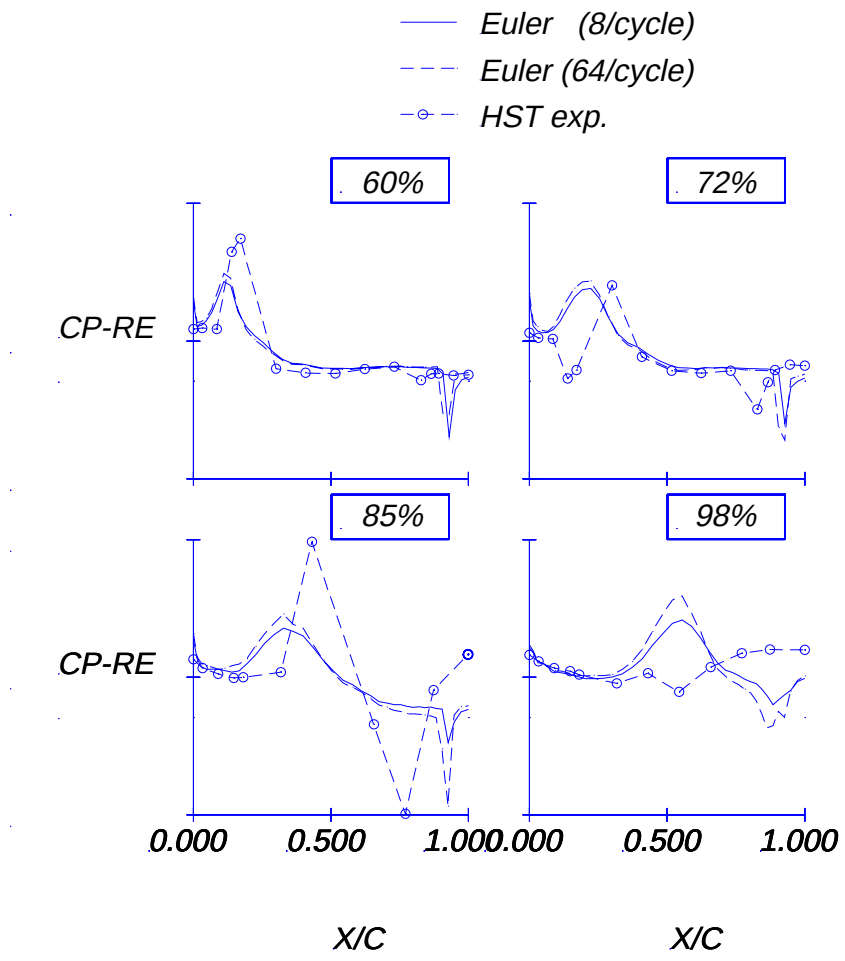

Fig. 14 Comparison of real part of experimental and calculated first harmonic pressure distributions on wing of fighter type configuration at $M_\infty = 0.92$, $\alpha = 6.00$, $\alpha_{amp} = 0.50$

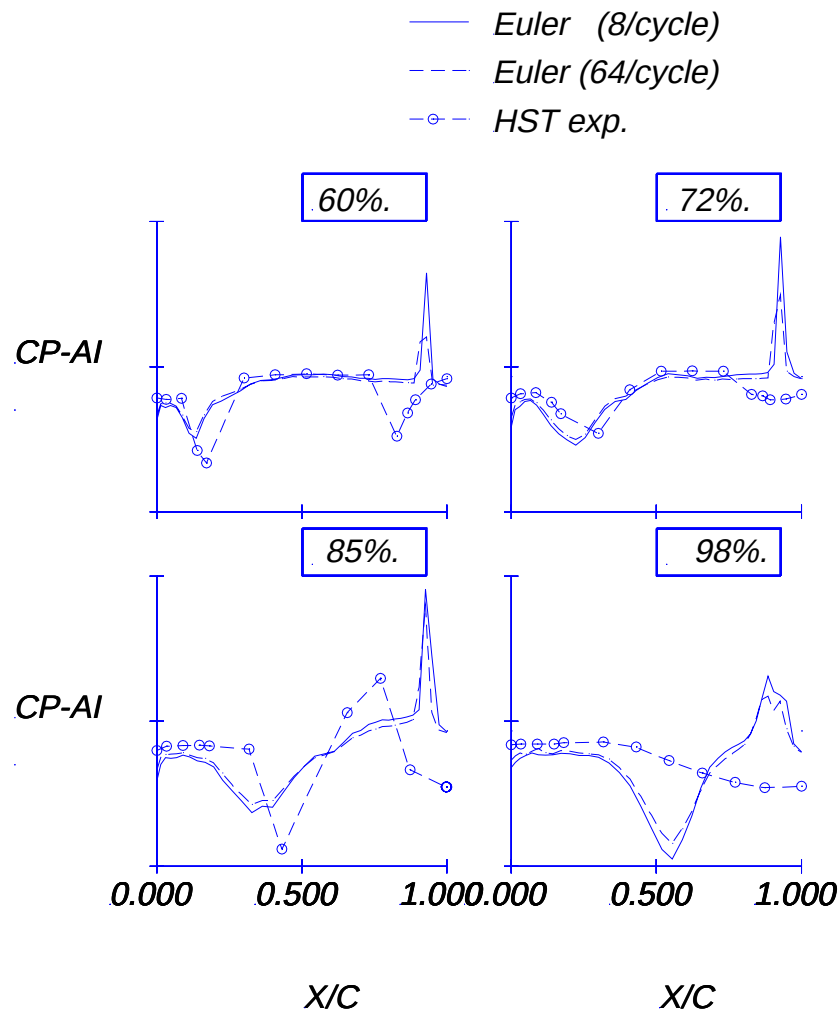

Fig. 15 Comparison of imaginary part of experimental and calculated first harmonic pressure distributions on wing of fighter type configuration at $M_\infty = 0.92$, $\alpha = 6.00$, $\alpha_{amp} = 0.50$